Available online at www.sciencedirect.com
ScienceDirect
Ceramics International 35 (2009) 3131–3134
CERAMICS INTERNATIONAL
www.elsevier.com/locate/ceramint

Study on the synthesis of $Al_2W_2MoO_{12}$ by a simple stearic acid route and its negative thermal expansion property

Gui-Fang Xu, Qin-Qin Liu, Juan Yang *, Xiu-Juan Sun, Xiao-Nong Cheng

School of Material Science and Engineering, Jiangsu University, Zhenjiang, Jiangsu, 212013, PR China

Received 2 March 2009; received in revised form 10 March 2009; accepted 29 April 2009
Available online 10 June 2009

Abstract

The $Sc_2W_3O_{12}$-type negative thermal expansion material attracts an extensive interest because of its thermodynamic stability and great chemical flexibility. In this paper, nanostructured $Sc_2W_3O_{12}$-type negative thermal expansion material $Al_2W_2MoO_{12}$ was synthesized by a convenient method, the stearic acid method. The thermodynamic property of the precursor was studied by thermogravimetric and differential scanning calorimetric methods. The structure and the size of the resulted products were characterized by powder X-ray diffraction and transmission electron microscopy, respectively. The negative thermal expansion property was studied by high temperature powder X-ray diffraction. Results show that nanostructured $Al_2W_2MoO_{12}$ powders with average size about 10 nm were first synthesized here by the stearic acid method and the nanoparticles would be rearranged to form large rods by prolonging the heat-treatment time. The obtained nanoparticles exhibited negative thermal expansion property in the temperature range of 20–600 °C.

Keywords: A. Powders: chemical preparation; B. Grain size; C. Thermal expansion

1. Introduction

In general, most solid crystals expand by increasing the temperature. On the contrary, the crystals that show a negative thermal expansion (NTE) property are rare and are known only in several oxide systems [1–4]. The most promising NTE material is ZrW_2O_8 due to its isotropic negative thermal expansion property over a large temperature range including room temperature (0.3–1050 K) [5–7]. Unfortunately for practical use, there are some drawbacks. ZrW_2O_8 is only thermodynamically stable at high temperatures, which makes it difficult to synthesise [8]. Due to the α-to-β phase transition, the expansion curve shows a discontinuity around 430 K and it makes the change of the linear expansion coefficient from −8.8 to $-4.9 \times 10^{-6}\ K^{-1}$ [9,10]. Moreover, ZrW_2O_8 undergoes a phase transition from cubic to orthorhombic structure at 0.21 GPa that is not reversible, which leads to problems during the processing and utilizing of composites filled with ZrW_2O_8 under pressure [11–13].

The $Sc_2W_3O_{12}$-type NTE material attracts interest because of its thermodynamic stability compared with ZrW_2O_8, which makes it easier to synthesis [14,15]. More remarkably, it shows great chemical flexibility, because the Sc atom can be replaced partly or totally by a trivalent transition metal atom or a lanthanide atom from Lu to Ho, and its thermal expansion coefficient can be changed to positive, zero or negative accordingly [16]. The study of $Sc_2W_3O_{12}$-type NTE material has gained considerable impetus recently due to its potential application in a large range of fields and $Al_2W_2MoO_{12}$ is one of the most intensely studied members. It can not only be used as a NTE material, acting as a filler in making composite to control the bulk thermal expansion coefficient, but also can be used as zero thermal expansion material which is desirable in optics, electronics and other fields, where exact positioning of parts is crucial [17,18].

The conventional method to prepare $Al_2W_2MoO_{12}$ is solid-state reaction using Al_2O_3, WO_3 and MoO_3 as raw materials. Products with large grain size will be obtained because of the high reaction temperature. But for actual application, the particle size might be an important consideration. Until now, there is little report on the control of the size of this kind material, especially on the preparing of nanometer sized material.

* Corresponding author. Tel.: +86 511 88780195; fax: +86 511 88791947.
E-mail address: yangjuan6347@ujs.edu.cn (J. Yang).

0272-8842/$36.00
doi:10.1016/j.ceramint.2009.04.028

Stearic acid method, which uses stearic acid as liganding solvent, is a convenient way for preparing nanostructured metal oxides, especially complex metal oxides, because nearly all the metal salts can be dissolved in melted stearic acid to form a uniform solution [19,20]. In this paper, the stearic acid route was adopted to synthesis nanostructured $Al_2W_2MoO_{12}$ powders. The structure and NTE property of $Al_2W_2MoO_{12}$ particles were investigated.

2. Experimental

Aluminum nitrate [$Al(NO_3)_3$], ammonium tungstate [$N_{10}H_{40}W_{12}O_{41}{\cdot}xH_2O$] and ammonium molybdate [$N_5H_{37}Mo_6O_{24}{\cdot}4H_2O$] were weighed according to the mole ratio of Al:W:Mo = 2:2:1. 10 g stearic acid was heated and melted. Into it, ammonium tungstate (1 mmol) and ammonium molybdate (1 mmol) were added slowly and the mixture was thoroughly stirred by a magnetic mixer. At the same time, ammonia was dropped continuously to the mixture till all the ammonium tungstate and ammonium molybdate were dissolved to form a transparent solution. Then aluminum nitrate (12 mmol) was added into the above solution and kept stirring for another 6 h. After natural cooling to RT, the precursor was ignited in air and then calcined at different temperatures for 6 h.

TG-DSC of the precursor was recorded on a NETZSCH-STA449.C thermogravimeter. The obtained products were characterized by powder X-ray diffraction using Rigaku D/max2500 X-ray diffractometer with Cu Kα radiation (λ = 0.15418 nm). The XRD data were collected with a scan speed of 5° (2θ) min^{-1} in the 2θ range from 10° to 50° by continuum scanning method. The samples' particle size was observed with JEOL JEM-2100 transmission electron micrograph.

3. Results and discussion

Fig. 1 shows the TG-DSC curves of the precursor gel of $Al_2W_2MoO_{12}$. It can be seen that there are two endothermic peaks in DSC curve. The first peak centered at 90.4 °C with about 6% weight loss may be caused by the desorption of water, and the second peak centered at 759.2 °C without weight loss is

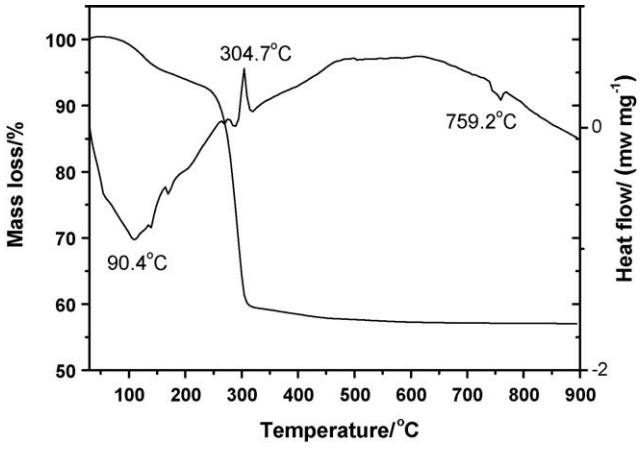

Fig. 1. TG-DSC curves of the precursor gel.

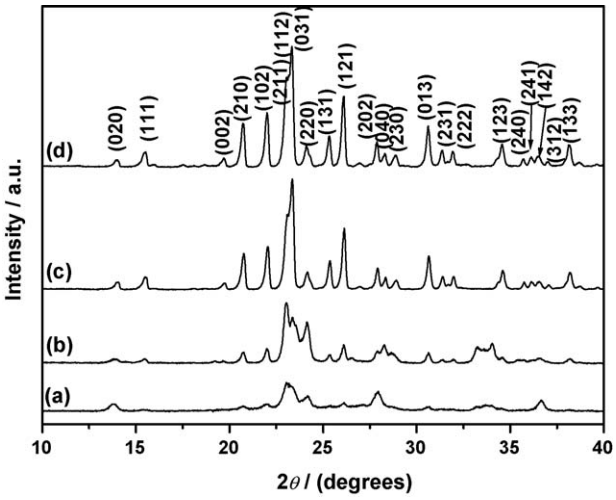

Fig. 2. XRD patterns of the (a) precursor powder ignited in air and the products calcined at a series of increasing temperatures of (b) 500 °C, 6 h; (c) 700 °C, 6 h; (d) 750 °C, 6 h.

attributed to the crystallization of $Al_2W_2MoO_{12}$. There is only one exothermic peak in DSC curve which centered at 304.7 °C with relative large weight loss (36.5%) in TG curve, which may be caused by the decomposition of the stearate and stearic acid. No further peak or weight loss was found up to 800 °C, suggesting that the crystallized $Al_2W_2MoO_{12}$ can be fabricated at about 759.2 °C.

To get $Al_2W_2MoO_{12}$ crystals, the precursor gel was ignited in air and then calcined in furnace at different temperatures. The changing process of the phase structure during the heat-treatment was recorded by XRD experiments and the results are shown in Fig. 2. In Fig. 2(a), it can be seen that the precursor powder is not amorphous, weak peaks assigning to $Al_2W_2MoO_{12}$ can be detected. This result seems different to the TG-DSC results and we consider that it might be caused by the different experimental conditions. In our experiment, the precursor gel was ignited in air to eliminate the organic solvent. Although the experiment was carried out at room temperature, the temperature inside the flame may be very high. The high temperature might facilitate the crystallization, so the following heat-treatment at different temperatures only make the crystallization complete. When heated at 500 °C, almost all the diffraction peaks resulting from $Al_2W_2MoO_{12}$ could be detected but with low intensity, as shown in Fig. 2(b). A single phase of $Al_2W_2MoO_{12}$ (JCPDS 24-1101) can be obtained when the sample was further heated at 700 °C for 6 h (Fig. 2(c)) and there is litter effect on the crystallinity by increasing the heat-treating temperature to 750 °C. It can be concluded that crystallized $Al_2W_2MoO_{12}$ powders can be formed at 700 °C using stearic acid method. Because of the broaden effect, (2 1 1), (1 1 2) and (0 3 1) peaks cannot be distinguished from each other as shown in Fig. 2(c) and (d). The obvious broaden of the diffraction peaks indicates that nanometer sized products might be obtained.

Fig. 3(a) shows the TEM image of the $Al_2W_2MoO_{12}$ powders obtained at 700 °C for 6 h. The average grain size is

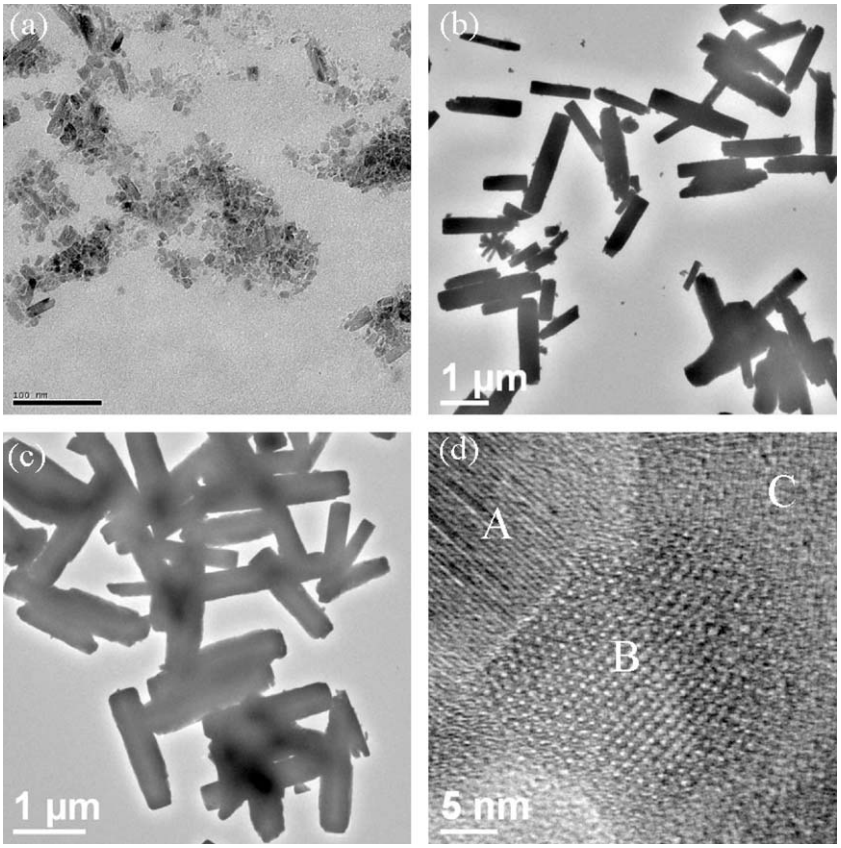

Fig. 3. (a) TEM image of $Al_2W_2MoO_{12}$ obtained at 700 °C for 6 h, (b) TEM image of $Al_2W_2MoO_{12}$ obtained at 700 °C for 12 h, (c) TEM image of $Al_2W_2MoO_{12}$ obtained at 700 °C for 18 h, and (d) HRTEM image of $Al_2W_2MoO_{12}$ rod.

about 10 nm and the particles are showing rod-like or plate-like morphology. The low reaction temperature and short reaction time resulted in the small grain size. By prolonging the heat-treatment time, it can be seen that the nonoparticles were rearranged to form large rods as shown in Fig. 3(b) and there are still some small particles around. When the heat-treatment time was prolonged to 18 h, the small particles were disappeared and large rods with average size of 400 nm × 2 μm became prominent (Fig. 3(c)). Fig. 3(d) shows the HRTEM image recorded from one of the rods in Fig. 3(c). By careful analysis, it can be found that the fringe pattern is not uniform and can be divided into many regions, such as A, B, C area marked in Fig. 3(d). It clearly reveals that the whole rod is not a single crystal and is composed of many tiny single crystals growing simultaneously and the area B is a small particle attached on the surface of the rods.

The NTE property of the obtained $Al_2W_2MoO_{12}$ was investigated. The lattice constants of $Al_2W_2MoO_{12}$ at different temperatures are collected by XRD and calculated by Jade5.0 software using $Al_2W_3O_{12}$ as model. The lattice constant of $Al_2W_2MoO_{12}$ at room temperature is $a = 0.9147$ nm, $b = 1.2602$ nm, $c = 0.9065$ nm and $V = 1.044$ nm^3. The temperature dependence of the a, b, and c axes and cell volume of $Al_2W_2MoO_{12}$ is shown in Fig. 4. It can be found that there are obvious interrupt changes in the curves of a axis and c axis at 600 °C in Fig. 4(A). In the temperature range of 20–600 °C, all the lattice constants of these three axes will decrease with increasing temperature and the thermal expansion coefficient of a axis, b axis, c axis and cell volume are -1.22×10^{-5}, -4.54×10^{-6}, -1.02×10^{-5} and -2.63×10^{-5} K^{-1}, respectively. But from 600 to 900 °C, the lattice constant of a axis and c axis will increase with increasing temperature while the lattice constant of b axis still decrease. The cell volume (Fig. 4(B)) showed the similar behavior as that of a and c axes, which decreases with increasing temperature from 20 to 600 °C and increases with increasing temperature from 600 to 900 °C. The experiment has been repeated twice and got the same results. This phenomenon is different from that reported in literature [21]. Usually, thermal expansion coefficient of a axis, b axis, c axis and cell volume of $Al_2W_3O_{12}$ single crystal obtained by modified Czochralski method are -1.69×10^{-6}, 8.31×10^{-6}, -0.15×10^{-6} and 1.17×10^{-6} K^{-1} when tested by TMA method. The difference might be caused by the size and different crystal structure resulted from the doping effect and different preparation method. To find the reason of the interrupt change of the lattice constants, the obtained powders were heat-treated at 500 and 600 °C and the XRD patterns are shown in Fig. 5. By careful comparison, one may notice that the relative intensity of peaks (2 1 0), (1 0 2), (2 1 1), (0 3 1), (0 4 0) are different between the two patterns, indicating that the crystal might undergo preferred growth at 600 °C and the detailed study are in progress now.

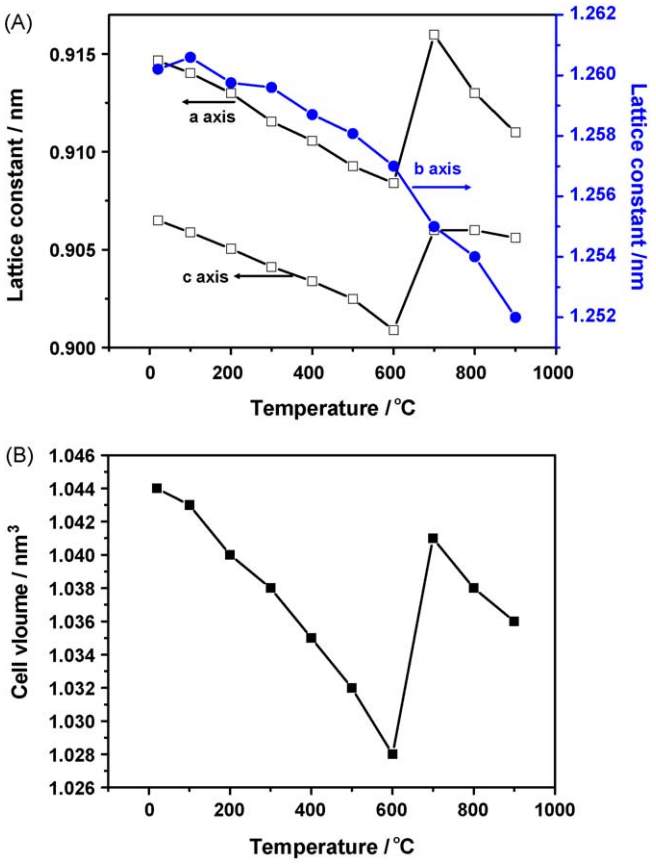

Fig. 4. Temperature dependence of (A) lattice constant of $Al_2W_2MoO_{12}$ and (B) cell volume of $Al_2W_2MoO_{12}$.

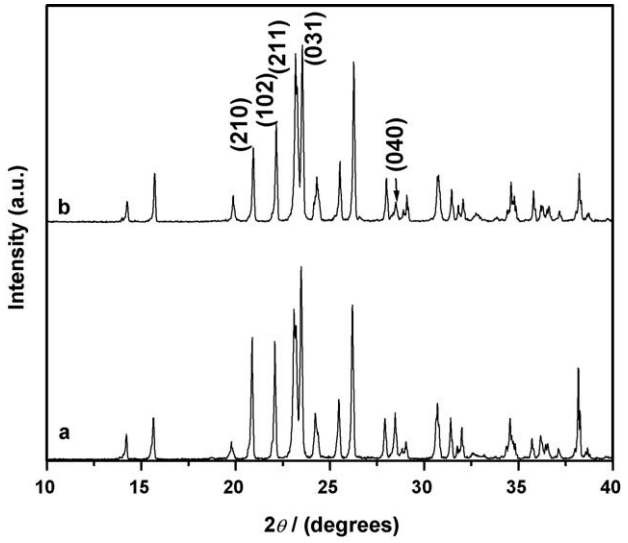

Fig. 5. XRD patterns of $Al_2W_2MoO_{12}$ collected at different temperatures: (a) 500 °C and (b) 600 °C.

4. Conclusions

Stearic acid method was proven to be a convenient way to prepare nanostructured $Al_2W_2MoO_{12}$ powders and the average particle size was about 10 nm. The obtained products showed NTE property in the temperature range of 20–600 °C. The thermal expansion coefficient of *a* axis, *b* axis, *c* axis and cell volume were -1.22×10^{-5}, -4.54×10^{-6}, -1.02×10^{-5} and $-2.63 \times 10^{-5}\ K^{-1}$, respectively. Compared with conventional solid-state method, stearic acid method is more rapid, convenient and general. It is an effective technique to produce complex metal oxides and may be popularized to the preparation of various $Sc_2W_3O_{12}$-type NTE materials.

References

[1] A.W. Sleight, Compounds that contract on heating, Inorg. Chem. 37 (12) (1998) 2854–2860.
[2] J.S.O. Evans, Negative thermal expansion materials, J. Chem. Soc., Dalton Trans. (1999) 3317–3326.
[3] A.K.A. Pryde, K.D. Hammonds, M.T. Dove, V. Heine, J.D. Gale, M.C. Warren, Origin of the negative thermal expansion in ZrW_2O_8 and ZrV_2O_7, J. Phys.: Condens. Matter 8 (1996) 10973–10982.
[4] D.K. Seo, M.H. Whangbo, Symmetric stretching vibrations of two-coordinate oxygen bridges as a cause for negative thermal expansion in $ZrV_xP_{2-x}O_7$ and AW_2O_8 (A = Zr, Hf) at high temperature, J. Solid State Chem. 129 (1) (1997) 160–163.
[5] T.A. Mary, J.S.O. Evans, T. Vogt, A.W. Sleight, Negative thermal expansion from 0.3 to 1050 Kelvin in ZrW_2O_8, Science 272 (1996) 90–92.
[6] G. Ernst, C. Broholm, G.R. Kowach, A.P. Ramirez, Phonon density of states and negative thermal expansion in ZrW_2O_8, Nature 396 (1998) 147–149.
[7] A.P. Ramirez, G.R. Kowach, Large low temperature specific heat in the negative thermal expansion compound ZrW_2O_8, Phys. Rev. Lett. 80 (1998) 4903–4906.
[8] U. Kameswari, A.W. Sleight, J.S.O. Evans, Rapid synthesis of ZrW_2O_8 and related phases, and structure refinement of $ZrWMoO_8$, Int. J. Inorg. Mater. 2 (4) (2000) 333–337.
[9] Z. Hu, J.D. Jorgensen, S. Teslic, S. Short, D.N. Argyrious, J.S.O. Evans, A.W. Sleight, Pressure-induced phase transformation in ZrW_2O_8—compressibility and thermal expansion of the orthorhombic phase, Phys. B: Condens. Matter 241 (1997) 370–372.
[10] Y. Yamamura, N. Nakajima, T. Tsuji, Heat capacity anomaly due to the α-to-β structural phase transition in ZrW_2O_8, Solid State Commun. 114 (9) (2000) 453–455.
[11] T.R. Ravindran, A.K. Arora, T.A. Mary, High pressure behavior of ZrW_2O_8: grüneisen parameter and thermal properties, Phys. Rev. Lett. 84 (17) (2000), pp. 3879-3782.
[12] J.S.O. Evans, Z. Hu, J.D. Jorgensen, N.D. Argyriou, S. Short, A.W. Sleight, Compressibility, phase transitions, and oxygen migration in zirconium tungstate, ZrW_2O_8, Science 275 (1997) 61–65.
[13] C.A. Perottoni, J.A.H. da Jornada, Pressure-induced amorphization and negative thermal expansion in ZrW_2O_8, Science 280 (1998) 886–889.
[14] J.S.O. Evans, T.A. Mary, A.W. Sleight, Negative thermal expansion in a large molybdate and tungstate family, J. Solid State Chem. 133 (2) (1997) 580–583.
[15] J.S.O. Evans, T.A. Mary, A.W. Sleight, Negative thermal expansion in $Sc_2(WO_4)_3$, J. Solid State Chem. 137 (1) (1998) 148–160.
[16] J.Z. Tao, A.W. Sleight, The role of rigid unit modes in negative thermal expansion, J. Solid State Chem. 173 (2) (2003) 442–448.
[17] J.S.O. Evans, T.A. Mary, Structural phase transitions and negative thermal expansion in $Sc_2(MoO_4)_3$, Int. J. Inorg. Mater. 2 (1) (2000) 143–151.
[18] P.M. Forster, A. Yokochi, A.W. Sleight, Enhanced negative thermal expansion in $Lu_2W_3O_{12}$, J. Solid State Chem. 140 (1) (1998) 157–158.
[19] J. Yang, D. Li, X. Wang, X.J. Yang, L.D. Lu, Synthesis and microstructural control of nanocrystalline titania powders via a stearic acid method, Mater. Sci. Eng. A 328 (1–2) (2002) 108–112.
[20] J. Yang, D. Li, X. Wang, X.J. Yang, L.D. Lu, Rapid synthesis of nanocrystalline TiO_2/SnO_2 binary oxides and their photoinduced decomposition of methyl orange, J. Solid State Chem. 165 (1) (2002) 193–198.
[21] N. Imanaka, M. Hiraiwa, G. Adachi, H. Dabkowska, A. Dabkowski, Thermal contraction behavior in $Al_2(WO_4)_3$ single crystal, J. Cryst. Growth 220 (1–2) (2000) 176–179.